Open Access **Baghdad Science Journal** **P-ISSN: 2078-8665**
Published Online First: May, 2023 **2024, 21(1): 107-116** **E-ISSN: 2411-7986**

DOI: https://doi.org/10.21123/bsj.2023.7945

A Theoretical Investigation of Chemical Bonding of a Heterometallic Trinuclear Cluster Containing Iridium and Ruthenium: [(Cp*Ir) $(CpRu)_2$ (μ_3-H) (μ-H)$_3$] by QTAIM Approach

Ahlam Hussein Hassan* ***Muhsen Abood Muhsen Al-Ibadi***

Department of Chemistry, College of Science, University of Kufa, Najaf, Iraq.
*Corresponding author: ahlamh.aitufaily@student.uokufa.edu.iq
E-mails address: muhsen.alibadi@uokufa.edu.iq

Received 13/10/2022, Revised 27/1/2023, Accepted 29/1/2023, Published Online First 20/5/2023, Published 01/1/2024

This work is licensed under a Creative Commons Attribution 4.0 International License.

Abstract:

Numerous integral and local electron density's topological parameters of significant metal-metal and metal-ligand bonding interactions in a trinuclear tetrahydrido cluster [(Cp* Ir) $(Cp\ Ru)_2$ (μ_3-H) (μ-H)$_3$]**1** (Cp = η^5 -C_5Me_5), (Cp* = η^5 -C_5Me_4Et) were calculated and interpreted by using the quantum theory of atoms in molecules (QTAIM). The properties of bond critical points such as the delocalization indices δ (A, B), the electron density $\rho(r)$, the local kinetic energy density $G(r)$, the Laplacian of the electron density $\nabla^2\rho(r)$, the local energy density $H(r)$, the local potential energy density $V(r)$ and ellipticity $\varepsilon(r)$ are compared with data from earlier organometallic system studies. A comparison of the topological processes of different atom-atom interactions has become possible thanks to these results. In the core of the heterometallic tetrahydrido cluster, the Ru_2IrH_4 part, the calculations showed that there are no bond critical points (BCPs) or identical bond paths (BPs) between Ru-Ru and Ru-Ir. The distribution of electron densities is determined by the position of bridging hydride atoms coordinated to Ru-Ru and Ru-Ir, which significantly affects the bonds between these transition metal atoms. On the other hand, the results confirm that the cluster under study contains a 7c–11e bonding interaction delocalized over M_3H_4, as shown by the non-negligible delocalization index calculations. The small values for $\rho(b)$ above zero, together with the small values, again above zero, for Laplacian $\nabla^2\rho(b)$ and the small positive values for total energy density H(b), are shown by the Ru-H and Ir-H bonds in this cluster is typical for open-shell interactions. Also, the topological data for the bond interactions between Ir and Ru metal atoms with the C atoms of the cyclopentadienyl Cp ring ligands are similar. They show properties very identical to open-shell interactions in the QTAIM classification.

Keywords: Bonding analysis for the trinuclear cluster, DFT calculation, QTAIM approach, Topological properties, and Trinuclear tetrahydrido cluster.

Introduction:

Over the past years, several studies have been reported on the activation of transition metal clusters in inorganic and organometallic chemistry due to their possible uses in catalytic or stoichiometric reactivity[1, 2]. These cluster complexes, which differ from mononuclear complexes in reactivity, can coordinate with substrate molecules many times and form a multi-electron transfer to the substrate [3, 4]. In the polyhydrido clusters, the releasing of bridging hydrido ligands play an important spontaneously introducing multiple unoccupied coordination sites on the neighboring metal centers[5–7]. Based on the very high electron density at the transition metal atoms of the polyhydrido clusters having cyclopentadienyl ligands, Suzuki et al.[8] argued that the reactivity was increased toward the splitting of

inactive chemical bonds, such as the C−C and C−H bonds of alkanes. In terms of computational methods, Bader's "theory of atoms in molecules (QTAIM)"[9, 10] simulations can be used to study the bonding and predict the properties of molecular structures[11, 12]. The key concept in the QTAIM theory is the distribution function of the electron density $\rho(r)$[13, 14]. The topological properties of $\rho(r)$ and its derivatives can play an important role in the concept of the metal-ligand and metal-metal interaction in organometallic compounds through valence bonds and non-valence interactions[14–16]. Unfortunately, the topology of the electron density in trinuclear heterometallic clusters having Iridium transition metals is still not fully understood. Therefore, to offer a rather satisfying interpretation of the bonding interactions in these important classes of clusters, more QTAIM studies are needed. This work aims to study the bonding by analyzing the electron density distributions and comparing different topological indicators for Ru-Ir, Ru-Ru, Ir-H, Ru-H, Ru-C, and Ir-C bonds in trinuclear heterometallic tetrahydrido cluster: [(Cp* Ir) (Cp Ru)$_2$ (μ_3-H) (μ-H)$_3$]**1** (Cp = η^5 -C_5Me_5), (Cp* = η^5 -C_5Me_4Et) [17], as displayed in Fig. 1. Also, the bridging hydride ligands in the trinuclear heterometallic cluster can be used as a model to study the influence of the bridging hydride atoms on the different Ru-Ru and Ru-Ir interactions. This study presents an excellent chance to investigate the topological characteristics of various bonding interactions inside this cluster.

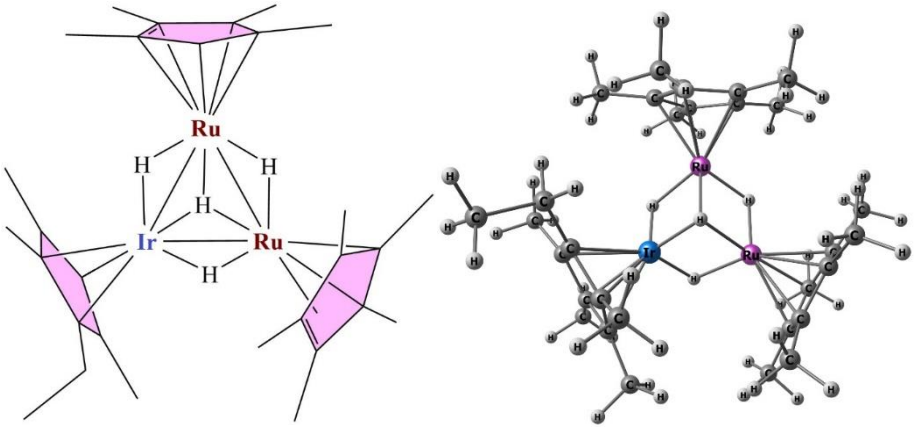

(I) (II)

Figure 1. I) Two-dimension structure of cluster 1 by ChemDraw program, (II) Three-dimension structure of geometrical optimization by chemcraft program.

Computational Methods

In this work, the DFT calculations for heterometallic tetrahydrido cluster **1** were done with the GAUSSIAN09[18] program and PBE1PBE functional[19]. In this study, we used the X-ray diffraction structure for this cluster**,** found by Suzuki and his co-workers [17], as a basis for geometrical optimization. The LANL2DZ basis set was used to calculate the metal atoms Ru and Ir, while the remaining atoms were described using a 6-31G (d, p) basis set [8, 20]. For the QTAIM calculations, we have used the AIM2000 program package [21]. The PBE1PBE density functional was used to perform these calculations on the theoretically optimized geometries. The large all-electron "well-tempered basis set" WTBS[22] was used for the Ru and Ir atoms, while the 6-31G (d, P) basis set was used for the remaining atoms[23, 24].

Results and Discussion:

Electron Density Topological Analysis

In the present paper, we first investigate the presence of bonding interactions in the trinuclear heterometallic tetrahydrido cluster **1** [(Cp* Ir) (Cp Ru)$_2$ (μ_3-H) (μ-H)$_3$] by using the QTAIM approach.

Applying this method to cluster **1** gives the complete set of bond critical points (BCPs) together with the bond paths (BPs) that relate the bonded atoms and ring critical points (RCPs). Fig. 2 presents the molecular graph of the cluster.

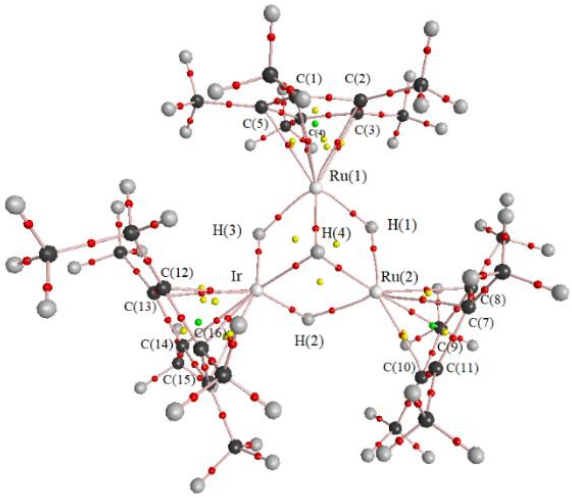

Figure 2. Molecular graph of the trinuclear heterometallic tetrahydrido cluster 1, where highlights gray lines represent (BPs bond pathways), small red circles represent (BCP critical bonding points between two atoms), yellow circles represent (ring critical points RCPs) and green circles represent (critical cage CCPs).

The BCPs and their BPs for the Ir-H, Ru-H, C-H, Ir-C, Ru-C, and C-C bonds were found using the molecular graph. Remarkably, the Ru_2IrH_4 core has no BCPs and BPs between the hydride-bridge transition metal atoms, Ir, Ru (1), and Ru (2). Then, we can assume that no direct Ru-Ru and Ru-Ir bonding exists[25] .Other ligands in bridging sits, such as carbonyl[26, 27], Borylenes[28], and Alkynes[29], have also shown this loss of M-M bond paths. Furthermore, RCPs located slightly closer to the geometrical centers of each Ru1-μ_2H1-Ru2-μ_3H4, Ru2-μ_2H2-Ir-μ_3H4, Ru1-μ_2H3-Ir-μ_3H4, and Cp ligands were observed for cluster **1**. A significant point of interest in this cluster is no direct bond-bond interaction between the transition metal atoms because no bond critical points and bond paths are observed between the metal atoms. The absence of bond paths (BCPs) hence, has no direct bonding interaction between these Ru-Ru and Ru-Ir metallic atoms.

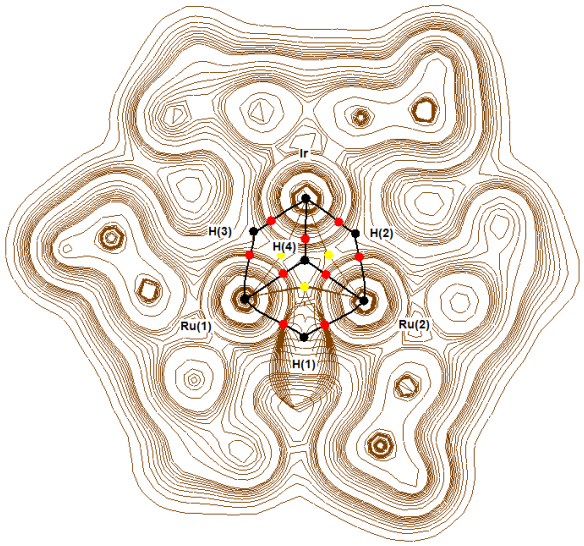

Figure 3. Gradient trajectories in the Ir-H(2)-Ru(2)-H(1)-Ru(1)-H(3) with H(4) plane mapped on an electron density plot, with atomic basins (BP's) and (BCP's).

In Fig. 3, a gradient map for core plane Ru(1)-H(1)-Ru(2)-H(3) and (μ_3-H) with Ru(1), Ru(2), and Ir, all bond critical points and pond paths with the atomic basins in the chosen planes are seen. In addition, the electron density distribution is very similar. It shows a significant charge density distribution around transition metal atoms Ru and Ir but no BCPs and BPs between Ru1-Ru2, Ru1-Ir, and Ru2-Ir. The BPs and BCPs located between Ru1-H, Ru2-H, and Ir-H are also shown.

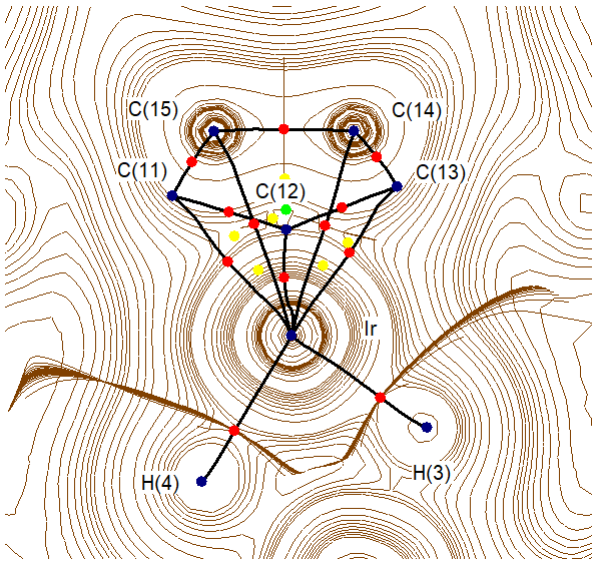

Figure 4. Gradient trajectories in the Cp ligand-Ir plane with atomic basins (BCP's) and (BP's).

Fig. 4 shows the BPs, BCPs, and RCPs associated with the CP* ligand attached to the Iridium atom and electron density's gradient map in this plane. The BCPs and BPs, found between Ir with the five carbons CP* atoms (C(11), C(12), C(13), C(14), and C(15)), located in and out of this plane, can also be observed. Additionally, H(1) and H(3) are shown on this plane.

Atoms in Molecules Analysis

The computed topological properties of the interactions between coordination bonds in the trinuclear heterometallic tetrahydrido cluster **1** are summarized in Table 1.

Table 1. The topological parameters at BCPs [(ρ_b) electron density, ($\nabla^2\rho_b$) Laplacian, (H_b) ratio of total energy density, (G_b) ratio of kinetic energy density, (V_b) viral energy density, and (εb) ellipticity].

Bond	ρ_b(eÅ^{-3})	$\nabla^2\rho_b$(eÅ^{-5})	G_b(he^{-1})	H_b(he^{-1})	V(he^{-1})	ε_b
Ru1-H1	0.092	0.188	0.079	-0.032	-0.112	0.162
Ru1-H3	0.076	0.188	0.069	-0.022	-0.091	0.224
Ru1-H4	0.056	0.170	0.053	-0.011	-0.063	0.133
Ru2-H1	0.094	0.190	0.081	-0.033	-0.114	0.136
Ru2-H2	0.075	0.189	0.068	-0.021	-0.090	0.264
Ru2-H4	0.055	0.170	0.053	-0.010	-0.063	0.122
Ir-H2	0.113	0.188	0.094	-0.047	-0.141	0.088
Ir-H3	0.113	0.186	0.094	-0.047	-0.141	0.092
Ir-H4	0.090	0.198	0.080	-0.031	-0.111	0.049
Ru1-C_{CP}[a]	0.080	0.254	0.083	-0.019	-0.102	1.258
Ru2-C_{CP}[a]	0.082	0.252	0.083	-0.020	-0.104	2.031
Ir-C_{CP*}[a]	0.078	0.252	0.081	-0.018	-0.099	1.561
C_{CP}-C_{CP}[a]	0.284	-0.682	0.091	-0.262	-0.353	0.225

[a] Average values.

M-M Interactions in Clusters 1

Bader's quantum theory of atoms in molecules approach is a powerful tool to provide information about atoms and the nature of chemical bonding interaction[30, 31]. Based on the QTAIM theory[32], the investigation of topological properties like "the electron density ρ_b, the Laplacian of electron density $\nabla^2\rho_b$, and the total energy density H_b at the BCPs" are a helpful tool for the classification of chemical bonds[33, 34].

From the literature, the calculated values of negative values of $\nabla^2\rho_b$ and H_b and large values of $\rho_b(r)$ are typical of shared or open-shell (covalent) interactions. Small values of ρ_b, positive values of $\nabla^2\rho_b$, and H_b are typical of closed shell (ionic or Van der Waals) interactions. The total energy density $H_b(r)$ is defined according to Eq. 1:

$$H_b(r) = G_b(r) + V_b(r) \quad \ldots\ldots\ldots\ldots 1$$

Where $G_b(r)$ and $V_b(r)$ are the kinetic and potential energy densities have been identified as a more appropriate index than Laplacian to characterize an interaction[35]. The important point for M-M (Ru-Ir and Ru-Ru) interactions is the total absence of any BCPs between any pair of transition metal atoms, which are bridged by hydride ligands. Thus, according to these results, we may say that there is no localized electron density between the Ru…Ru

or Ru…Ir interactions. According to the QTAIM model, defining and characterizing a chemical bond is associated with a found bond critical point[36]. The topological M…M (Ru…Ir and Ru…Ru) bonds were destroyed when the metal transition atoms were spanned by μ_2-H and μ_3-H bridging hydride ligands (strong interaction). Depending on what was mentioned above, we conclude that there is no bond between transition metal atoms in this cluster. The absence of BCP between the metal-metal atoms has been observed, such as in bridged M…M interaction in the compounds studied by Van der Maelen et al. $[Mn_3(\mu\text{-}H)_3(CO)_{12}]$, $[Tc_3(\mu\text{-}H)_3(CO)_{12}]$, $[Re_3(\mu\text{-}H)_3(CO)_{12}]$[37] and bridged Os…Os in clusters $[Os_3(l\text{-}H)(l\text{-}Cl)(CO)_{10}]$ and $[Os_3(l\text{-}H)(l\text{-}OH)(CO)_{10}]$ [38]. However, the BCP and its BP between the metal-metal atoms have also been observed when there are strong ligand bridging interactions (μ^2-S), as in the case of Mo-Mo in the complex $[Mo_3\ (\mu^2\text{-}S)\ (\mu^2\text{-}S)_3\ Cl_3(PH_3)_6]^+$ (Feliz et al.[39]).

M-H Interactions in Cluster 1

For Ir-H and Ru–H interactions, according to Table. 1, the electron density values at the BCPs are small, >1, within the range 0.055 to 0.113 eÅ^{-3}, though the Laplacian values are also small, again >1, 0.170 to 0.193 e Å^{-5}. These results added to the negative values for H_b, which are in the range of -0.010 to -0.047 he^{-1}, enforce us to assume that the Ru-H and Ir-H interactions are typical of the shared or open-shell (covalent) interactions in line with that of a typical open-shell bond (intermediate between ionic and covalent bonds)[10,34,40]. However, the central hydride bridge's M-H4(μ3) bonds exhibit observable topological properties. For instance, it is lower in electron density and higher in the H_b values. In addition, the values, slightly greater than zero of the ellipticity for each of the Ru-H and Ir-H bonds are typical of the straight bonding interactions between M and H atoms.

The Laplacian map computed to plane containing (Ru_2IrH_4) is very useful for analyzing the M..M and M-H interactions, as shown in Fig. 5. The pseudo-octahedral coordination of the Ru and Ir atoms in this cluster is further evident in this figure, demonstrating how their valence shell charge depletion (VSCD) is almost perfectly cubic. Also, the VSCDs of hydrido bridge ligands are directed toward the middle distance of the two transition atoms they are bonded to. The reasons for the absence of BPs and BCPs in the shape of the Laplacian distribution between Ru...Ru and Ru…Ir suggests that there are no bonding electron pairs between these transition metal atoms.

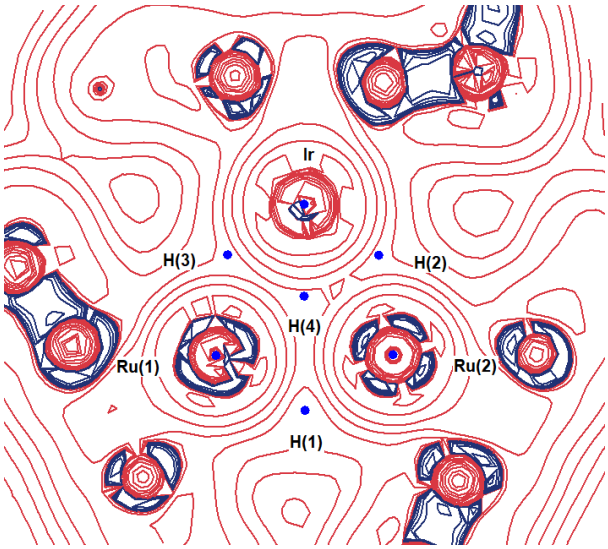

Figure 5. Laplacian map showing the electron density of Ir -H(2)-Ru(2)-H(1)- Ru(1) -H(3) with H(4) plane in the trinuclear cluster 1.

M-Cp Interactions in Cluster 1

The five BPs were given their BCPs between Ir and C atoms of the Cp* ligand, which is a most notable aspect of the topological analysis for the Ir-C interactions in this cluster, as shown in Fig. 6. Thus, it is fair to say that there is a real chemical bonding between Ru metal and the carbon atom of Cp* ligands, not just 'interactions' as previously found in other M-Cp interactions [41]. The calculated topological parameters for Ru-C and Ir-C bonds are summarized in Table 1. From these data, we argue that the Ru-C, and Ir-C bonds interactions, belong to the transit closed-shell category with positive values for ρ_b (0.078 - 0.082e Å^{-3}), the $\nabla^2\rho_b$'s small and positive values in the range of (0.252 to 0.254 e Å^{-5}) and negative, near-zero values of H_b (-0.018 to -0.020 he^{-1}). These numbers are consistent with the values that have previously been published in the literature[42]. Finally, the calculated ellipticities for the M-C bonds showed that the ellipticities average

values of Ir-Cp* interactions (1.561) are in most cases lower than the Ru-Cp bonds (1.258-2.031). The M-C bonds have a л character, according to computed large values for the ellipticities, which is compatible with past findings based on the MO theory[43].

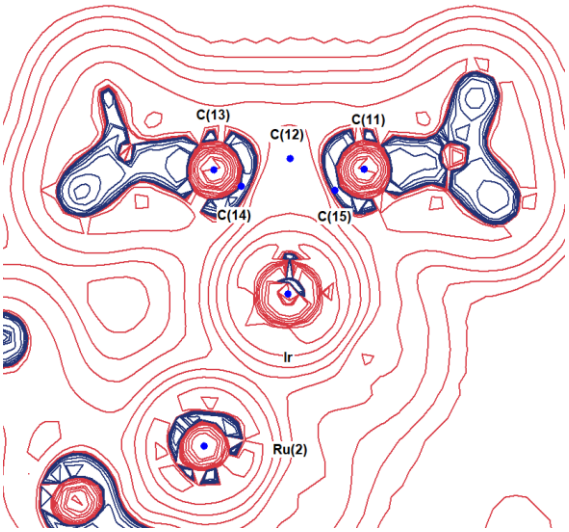

Figure 6. Laplacian map showing the electron density in the Ir-Cp* plane.

Delocalization Indices.

The delocalization index, δ(A, B), is one of the best tools to estimate the number of delocalized electron pairs between two atoms[43, 44]. Therefore, as listed in Table 2, we calculated these indices as a tool to analyze a multicenter bonding in this cluster from one side and to describe different M…M interaction modes from another side[38].

Table 2. Delocalization indices of atom pairs interactions in cluster 1.

Atom pairs (A and B)	δ (A, B)	Atom pairs (A and B)	δ (A, B)
Ru1-H1	0.536	Ir-H4	0.492
Ru1-H3	0.435	Ru1-C_{CP}[a]	0.425
Ru1-H4	0.319	Ru2-C_{CP}[a]	0.482
Ru2-H1	0.549	Ir-C_{CP*}[a]	0.410
Ru2-H2	0.431	Ru1...Ru2	0.369
Ru2-H4	0.316	Ru1…Ir	0.334
Ir-H2	0.569	Ru2…Ir	0.301
Ir-H3	0.625		

[a] Average values.

The computed delocalization indices of M...M interaction values for this cluster (0.301-0.369) are higher than the reported hydride-bridged M...M nonbonding interaction values obtained in numerous other published QTAIM investigations. These studies showed that BCPs and BPs are not located in several bridged M...M nonbonding interactions giving δ(A, B) values of 0.169-0.246, 0.177, and 0.202 for "$[Ru_3(\mu\text{-}H)_2(\mu^3\text{MeImCH})(CO)_9]$"[45], "$[Os_3(\mu\text{-}H)(\mu\text{-}Cl)(CO)_{10}]$"[38], and "$[Ru_3(\mu\text{-}H)(\mu_3\text{-}\kappa^2\text{-Hamphox-N, N})(CO)_9]$"[3], respectively.

Alternatively, the calculated values of delocalization indices of the nonbonding M...M interaction of cluster **1** are comparable in magnitude to values found in many bridged M-M bond interactions (weak metal-metal interaction) such as Os-Os interactions of the cluster "$[Os_3(\mu\text{-}H)_2(CO)_{10}]$" [38] (0.362). As a result, it is possible to say the value of the δ(A–B) for each of the M…M bonds in cluster **1** is large enough to confirm that the M...M interaction is closer to the composition of its bond (weak metal-metal interaction) than its absence[38,46]. The values found for δ(M–H) in cluster

1 (0.316-0.625) are like those obtained, for instance, for Os–H (0.426-0.449) and Ru–H (0.474) bonds of the clusters mentioned above [38,45]. Also, they are lower than that calculated for the complex terminal hydrido $[CrH(CO)_5]^-$ (0.59) [47] and close to $[(\mu\text{-}H)Cr_2(CO)_{10}]^-$ (0.38), especially the central hydride bridge δ (M-H4) values. In summary, δ(M–H) calculations suggest that each of the four M-H bonds in cluster **1** has just half a shared pair electron. Based on the sum of the δ(A–B) for the interactions in the core part $Ru_2Ir(\mu\text{-}H)_3(\mu_3\text{-}H)$ of cluster **1** (5.276), thus a multicenter 7c–11e interaction in this part of the molecule is suggested to explain the bonding in this cluster.

Conclusions:

In this study, QTAIM method was used to investigate the bonding in the trinuclear heterometallic tetrahydrido cluster [(Cp* Ir) (Cp Ru)$_2$ (μ_3-H) (μ-H)$_3$]**1**. The metal-ligand and metal-metal bond critical points parameters *ρ(r)*, $\nabla^2\rho(r)$, *G(r), H(r), V(r)*, and δ(A, B), as well as ellipticity, are correlated with the computed data in the former organometallic systems studies. These results allowed an excellent comparison of the topological properties of various atom-atom interactions. Our calculations suggest that a multicentre 7c–11e type exists in the bridged core part, $Ru_2Ir(\mu_3\text{-}H)(\mu\text{-}H)_3$. Most intriguingly, the presence of bridging hydride ligands affects the electron density distribution of Ru...Ru and Ru...Ir interactions, for which no direct bonding has been observed due to the absence of BCPs and their BPs between these transition metals. The calculated topological properties of the Ru-H, Ir-H, Ru-Cp, and Ir-Cp bonds indicate that they are all typical open-shell bonds.

Acknowledgment:

The cooperation of the quantum group at Kufa University is appreciated.

Authors' declaration:

- Conflicts of Interest: None.
- We hereby confirm that all the Figures and Tables in the manuscript are ours. Besides, the Figures and images, which are not ours, have been given the permission for re-publication attached with the manuscript.
- The author has signed an animal welfare statement.
- Ethical Clearance: The project was approved by the local ethical committee in University of Kufa.

Authors' contributions statement:

Manuscript preparation, computational analysis, and final editing were conducted by A.H. While manuscript review was made by M.A. All authors read and agreed to the published version of the manuscript.

References:

1. Zhang X. Computational insights into organic and organometallic catalysis. University of Oxford. 2019. https://ethos.bl.uk/OrderDetails.do?uin=uk.bl.ethos.799939.
2. Chipman JA, Berry JF. Paramagnetic Metal–Metal bonded heterometallic complexes. Chem Rev. 2020; 120(5): 2409–2447; https://doi.org/10.1021/acs.chemrev.9b00540.
3. Muhsen Al-Ibadi MA, Taha A, Hasan Duraid AH, Alkanabi T. A theoretical investigation on chemical bonding of the bridged hydride triruthenium cluster: [Ru3 (μ-H)(μ3-κ2-hamphox-N,N)(CO)9]. Baghdad Sci J. 2020; 17(2): 488-93. https://doi.org/10.21123/bsj.2020.17.2.0488
4. Chikamori H, Tahara A, Takao T. Transformation of a μ3-Benzyne ligand into phenol on a cationic triruthenium cluster supported by a μ3-Sulfido ligand. Organometallics. 2018; 38(2): 527-35. https://doi.org/10.1021/acs.organomet.8b00832
5. Takao T, Suzuki H, Shimogawa R. Syntheses and properties of triruthenium polyhydrido complexes composed of 1,2,4-tri-tert-butylcyclopentadienyl and p-Cymene ruthenium units. Organometallics. 2021; 40(9): 1303-13. https://doi.org/10.1021/acs.organomet.1c00094
6. Daniels C, Gi E, Atterberry B, Blome-Fernández R, Rossini A, Vela J. Phosphine ligand binding and catalytic activity of group 10–14 heterobimetallic complexes. Inorg Chem. 2022; 61(18): 6888-97. https://doi.org/10.1021/acs.inorgchem.2c00229
7. AL-Nafee, M. Metal-Metal bonding in poly-metallic systems. PhD thesis, University of Oxford, 2019. https://ora.ox.ac.uk/objects/uuid:95f6c115-e1de-40b3-8f0b-eb6ce93e78b0
8. Al-Ibadi MAM, Alkurbasy NE, Alhimidi SRH. The topological classification of the bonding in[(Cp'Ru)2 (Cp'Os)(μ3-N)2(μ-H)3] cluster. AIP Conf Proc. 2019; 2144(1): 20009. https://doi.org/10.1063/1.5123066.
9. Bader RFW. Atoms in molecules a quantum theory. Oxford science publications. Clarendon Press; 1900.

438p. https://books.google.iq/books?id=up1pQgAACAAJ
10. Al-Kirbasee NE, Alhimidi SRH, Al-Ibadi MAM. QTAIM study of the bonding in triosmium trihydride cluster [Os3(μ-H)3(μ3-É2-CC7H3(2-CH3)NS)(CO)8]. Baghdad Sci J. 2021; 18(4): 1279-85. https://doi.org/10.21123/BSJ.2021.18.4.1279.
11. Rampino S. Chemistry at the Frontier with Physics and Computer Science. Elsevier; 2022. Chap 14, The atom and the bond; p. 151-66. https://doi.org/10.1016/b978-0-32-390865-8.00024-6
12. Wen L, Li G, Yang LM, Pan H, Ganz E. The structures, electronic properties, and chemical bonding of binary alloy boron–aluminum clusters series B4Aln0/−/+ (n = 1–5). Mater Today Commun. 2020; 24(1): 100914. https://doi.org/10.1016/J.MTCOMM.2020.100914
13. Cheng X, Lei A, Mei TS, Xu HC, Xu K, Zeng C. Recent applications of homogeneous catalysis in electrochemical organic synthesis. CCS Chem. 2022; 4(4): 1120-52. https://doi.org/10.31635/ccschem.021.202101451.
14. Malloum A, Conradie J. QTAIM analysis dataset for non-covalent interactions in furan clusters. Data Br. 2022; 40(1): 107766. https://doi.org/10.1016/j.dib.2021.107766
15. van der Maelen JF, Ceroni M, Ruiz J. The X-ray constrained wavefunction of the [Mn(CO)4{(C6H5)2P-S-C(Br2)-P(C6H5)2}]Br complex: A theoretical and experimental study of dihalogen bonds and other noncovalent interactions Acta Crystallogr B Struct Sci Cryst Eng Mater. 2020; 76(5): 802-814. https://doi.org/10.1107/S2052520620009889
16. Attia AS, Alfallous KA, El-Shahat MF. A novel quinoxalinedione-bicapped tri-ruthenium carbonyl cluster [Ru3(μ-H)2(CO)6(μ3-HDCQX)2]: synthesis, characterization, anticancer activity and theoretical investigation of Ru–Ru and Ru–Ligand bonding interactions Polyhedron. 2021; 193(1): 114889. https://doi.org/10.1016/j.poly.2020.114889
17. Shima T, Sugimura Y, Suzuki H. Heterometallic trinuclear polyhydrido complexes containing ruthenium and a group 9 metal, [Cp*$_3$Ru$_2$M(μ$_3$-H)(μ-H)$_3$] (M = Ir or Rh; Cp* = η^5-C$_5$Me$_5$): Synthesis, structure, and site selectivity in reactions with phosphines. Organometallics. 2009; 28(3): 871–881. https://doi.org/10.1021/om8010432.
18. Frisch MJ, Trucks GW, Schlegel HB, Scuseria GE, Robb MA, Cheeseman JR, et al. Gaussian 09, program, Revision A.02. Gaussian, Inc. Wallingford 2016. https://gaussian.com/g09citation/
19. Hirva P, Haukka M, Jakonen M, Moreno MA. DFT tests for group 8 transition metal carbonyl complexes. J Mol Model. 2008; 14(3): 171-81.
20. Alhimidi SRH, Al-Ibadi MAM, Hasan AH, Taha A. The QTAIM approach to chemical bonding in triruthenium carbonyl cluster:[Ru3 (μ-H)(μ3-κ2-Haminox-N, N)(CO) 9]. J Phys. 2018; 1032(1): 12068.
21. Biegler-König F, Schönbohm J. AIM2000. J Comput Chem. 2002; 22(1): 545-559. https://doi.org/10.1002/1096-987X(20010415)22:5<545::AID-JCC1027>3.0.CO;2-Y.
22. Huzinaga S, Klobukowski M. Well-tempered Gaussian basis sets for the calculation of matrix Hartree-Fock wavefunctions. Chem Phys Lett. 1993; 212(3–4): 260–264. https://doi.org/10.1016/0009-2614(93)89323-A.
23. Al-Ibadi MAM, Oraibi DT, Hasan AH. The ruthenium-ruthenium bonding in bridged ligand system: QTAIM study of [Ru3(μ3-κ2-MeimCh) (μ-CO) (CO)9] complex. AIP Conf Proc. 2019; 2144(1): 20008. https://doi.org/10.1063/1.5123065
24. Adamo C, Barone V. Toward reliable density functional methods without adjustable parameters: The PBE0 model. J Chem Phys. 1999; 110(13): 6158.
25. Yang X, Chin RM, Hall MB. Protonating metal-metal bonds: Changing the metal-metal interaction from bonding, to nonbonding, and to antibonding. Polyhedron. 2022; 212(1): 115585. https://doi.org/10.1016/j.poly.2021.115585.
26. Cesari C, Bortoluzzi M, Forti F, Gubbels L, Femoni C, Iapalucci MC, et al. 2-D molecular alloy Ru–M (M = Cu, Ag, and Au) carbonyl clusters: synthesis, molecular structure, catalysis, and computational studies. Inorg Chem Published online September. 2022; 61(37): 14726–14741. https://doi.org/10.1021/ACS.INORGCHEM.2C02099
27. Ruiz J, Sol D, Garciá L, Mateo MA, Vivanco M, Van Der Maelen JF. Generation and tunable cyclization of formamidinate ligands in carbonyl complexes of Mn(I): An experimental and theoretical study. Organometallics. 2019; 38(4): 916–925. https://doi.org/10.1021/acs.organomet.8b00898
28. Flierler U, Burzler M, Leusser D, Henn J, Ott H, Braunschweig H, et al. Electron-density investigation of Metal–Metal bonding in the dinuclear “Borylene” complex [Cp(CO)$_2$Mn$_2$(μ-BtBu)]. Angew Chem Int Ed Engl. 2008; 47(23): 4321–4325. https://doi.org/10.1002/anie.200705257.
29. Overgaard J, Clausen HF, Platts JA, Iversen BB. Experimental and theoretical charge density study of

chemical bonding in a Co dimer complex. J Am Chem Soc. 2008; 130(12): 3834-43.

30. Domagała M, Lutyńska A, Palusiak M. Extremely Strong Halogen Bond. The Case of a Double-Charge-Assisted Halogen Bridge. J Phys Chem A. 2018; 122(24): 5484-92. https://doi.org/10.1021/acs.jpca.8b03735.
31. Prasad Kuntar S, Ghosh A, K. Ghanty T. Superstrong chemical bonding of noble gases with oxidoboron (BO+) and sulfidoboron (BS+). J Phys Chem A. 2022; 126(43): 7888–7900. https://doi.org/10.1021/acs.jpca.2c05554.
32. Korabel'nikov D V, Zhuravlev YN. The nature of the chemical bond in oxyanionic crystals based on QTAIM topological analysis of electron densities. RSC Adv. 2019; 9(21): 12020-12033. https://doi.org/10.1039/c9ra01403a.
33. Anil Kumar GN, Shruthi DL. The nature of the chemical bond in sodium tungstate based on ab initio, DFT and QTAIM topological analysis of electron density. Mater Today Proc Elsevier. 2021; 44(8): 3127-32. https://doi.org/10.1016/j.matpr.2021.02.810.
34. van der Maelen JF, Brugos J, García-Álvarez P, Cabeza JA. Two octahedral σ-borane metal (MnI and RuII) complexes containing a tripod κ3N,H,H-ligand: Synthesis, structural characterization, and theoretical topological study of the charge density. J Mol Struct. 2020; 1201(127217): 127217. https://doi.org/10.1016/j.molstruc.2019.127217.
35. F. Van der Maelen J. Topological analysis of the electron density in the carbonyl complexes M(CO)8 (M = Ca, Sr, Ba). Organometallics. 2019; 39(1): 132-41. https://doi.org/10.1021/acs.organomet.9b00699.
36. Gadre SR, Suresh CH, Mohan N, Kuznetsov ML. Molecules electrostatic potential topology for probing molecular structure bonding and reactivity. Molecules. 2021; 26(11): 3289. https://doi.org/10.3390/molecules26113289.
37. Van der Maelen JF, Cabeza JA. A topological analysis of the bonding in [M2(CO)10] and [M3(μ-H)3(CO)12] complexes (M = Mn, Tc, Re). Theor Chem Acc. 2016; 135(3): 1-11. https://doi.org/10.1007/s00214-016-1821-0.
38. Maelen JF van der, García-granda S, Cabeza JA. Theoretical topological analysis of the electron density in a series of triosmium carbonyl clusters: [Os3(CO)12], [Os3(μ-H)2(CO)10], [Os3(μ-H)(μ-OH)(CO)10] and [Os3(μ-H)(μ-Cl)(CO)10]. Comput Theor Chem. 2011; 968(1-3): 55-63. https://doi.org/10.1016/j.comptc.2011.05.003.
39. Feliz M, Llusar R, Andrés J, Berski S, Silvi B. Topological analysis of the bonds in incomplete cuboidal [Mo 3 S 4] clusters. New J Chem. 2002; 26(7): 844-50.
40. Nishide T, Hayashi S. Intrinsic dynamic and static nature of π···π interactions in fused benzene-type helicenes and dimers, elucidated with QTAIM dual functional analysis. J Nanomater. 2022; 12(3): 321. https://doi.org/10.3390/NANO12030321.
41. Van der Maelen JF, Gutiérrez-Puebla E, Monge A, García-Granda S, Resa I, Carmona E, et al. Experimental and theoretical characterization of the Zn—Zn bond in [Zn2 (η5-C5Me5) 2]. Acta Crystallogr B. 2007; 63(6): 862-8.
42. Helal SR, Al-Ibadi MAM, Hasan AH, Taha A. The QTAIM approach to chemical bonding in triruthenium carbonyl cluster: [Ru3 (μ-H)(μ 3-κ 2-Haminox-N,N)(CO)9]. J Phys Conf Ser. 2018; 1032(1): 12068. https://doi.org/10.1088/1742-6596/1032/1/012068.
43. Isaac C, Wilson C, Burnage A, Miloserdov M, Mahon M, Macgregor S, et al. Experimental and computational studies of ruthenium complexes bearing Z-Acceptor Aluminum-Based phosphine pincer ligands. Inorg Chem. 2022; 61(50): 20690–20698. https://doi.org/10.1021/acs.inorgchem.2c03665.
44. Bartashevich E v, Mukhitdinova SE, Tsirelson VG. Bond orders and electron delocalization indices for S–N, S–C and S–S bonds in 1,2,3-dithiazole systems. Mendeleev Commun. 2021; 31(5): 680-3. https://doi.org/10.1016/j.mencom.2021.09.029.
45. Cabeza JA, Van Der Maelen JF, Garcia-Granda S. Topological analysis of the electron density in the N-heterocyclic carbene triruthenium cluster [Ru3(μ-H)2(μ3- MeImCH)(CO)9] (Me2im = l,3-dimethylimidazol-2-ylidene). Organometallics. 2009; 28(13): 3666-72. https://doi.org/10.1021/om9000617.
46. Al-Ibadi MAM, Kzar KO. Theoretical study of Fe-Fe bonding in a series of iron carbonyl clusters [(μ-H)2Fe3(CO)9(μ3-As)Mn(CO)5], [Et4N] [(μ-H)2Fe3(CO)9(μ3-As)Fe(CO)4] and [Et4N][HAs{Fe2(CO)6(μ-CO) (μ-H)}{Fe(CO)4}] by QTAIM perspective. Egypt J Chem. 2020; 63(8): 2911-20. https://doi.org/10.21608/ejchem.2020.21235.2267.
47. Macchi P, Donghi D, Sironi A. The electron density of bridging hydrides observed via experimental and theoretical investigations on [Cr2(μ2-H)(Co) 10]-. J Am Chem Soc. 2005; 127(47): 16494-504. https://doi.org/10.1021/ja055308a

Open Access **Baghdad Science Journal** **P-ISSN: 2078-8665**
Published Online First: May, 2023 **2024, 21(1): 107-116** **E-ISSN: 2411-7986**

تحقيق نظري للارتباط الكيميائي لعنقود ثلاثي النوى غير متجانس يحتوي على الإيريديوم والروثينيوم: [(Cp* Ir) (Cp Ru)$_2$ (μ_3-H) (μ-H)$_3$] من خلال نهج QTAIM

احلام حسين حسن **محسن عبود محسن**

قسم الكيمياء، كلية العلوم، جامعة الكوفة، النجف الاشرف، العراق.

الخلاصة:

تم حساب وتفسيرالعديد من المعلمات الطوبولوجية الموقعية والمتكاملة لكثافة الإلكترون لتفاعلات ترابط المعادن مع المعدن والروابط المعدنية المهمة في المركب العنقودي رباعي النوى رباعي هيدريدو

[(Cp* Ir) (Cp Ru)$_2$ (μ_3-H) (μ-H)$_3$]**1** (Cp = η^5 -C_5Me_5), (Cp* = η^5 -C_5Me_4Et)

تم حسابها وتفسيرها بأستخدام نظرية الكم للذرات في الجزيئات (QTAIM). تمت مقارنة خصائص النقاط الحرجة للاواصر مثل مؤشرات إلغاء تحديد موقع الرابطة $\delta(A, B)$، كثافة الإلكترون $\rho(r)$ ، كثافة الطاقة الحركية الموقعية $G(r)$، Laplacian لكثافة الإلكترون $\nabla^2\rho(r)$ ، كثافة الطاقة الموقعية $H(r)$ ، وكثافة الطاقة الكامنة الموقعية $V(r)$ والإهليلجيه $\varepsilon(r)$ مع البيانات من دراسات الانظمة العضوية المعدنية السابقة. أصبحت مقارنة العمليات الطوبولوجية لتفاعلات (ذرة مع ذرة) المختلفة ممكنة بفضل هذه النتائج. ، تُظهر الحسابات في قلب مجموعة رباعي هيدريدو غير المتجانسة في الجزء Ru_2IrH_4 عدم وجود أي نقاط حرجة للاواصر (BCP) أو لمسارات اصرة متطابقة (BPs) بين Ru-Ru و Ru-Ir. وتم تحديد توزيع كثافات الإلكترون من خلال موضع تجسير ذرات هيدريد المنسقة مع Ru-Ru و Ru-Ir ، وهذا له تأثير كبير على تكوين الاواصر بين ذرات المعدن الانتقالي. من ناحية أخرى ، تؤكد النتائج أن الكتلة قيد الدراسة تحتوي على تفاعل ترابط 7c–11e غير محدد على M_3H_4 ، كما هو موضح في حسابات مؤشر إلغاء تحديد الموقع غير المهملة. وتظهر القيم الصغيرة لكثافة الإلكترون $\rho(b)$ فوق الصفر، جنبًا إلى جنب مع القيم الصغيرة ، مرة أخرى فوق الصفر، لـ $\nabla^2\rho(b)$ Laplacian والقيم الإيجابية الصغيرة لكثافة الطاقة الإجمالية $H(b)$، بواسطة روابط H-Ru و Ir-H في هذا المركب العنقودي نموذجا لتفاعلات الغلاف المفتوح أيضًا، تتشابه البيانات الطوبولوجية لتفاعلات الروابط بين ذرات المعادن Ir و Ru مع ذرات C من بروابط حلقة cyclopentadienyl Cp، وتُظهر خصائص مشابهة جدًا لتفاعلات الاغلفة المفتوحة وفق نهج حسابات QTAIM.

الكلمات المفتاحية: تحليل الترابط للكتلة ثلاثية النوى ، وحساب DFT ، طريقة QTAIM ، والخصائص الطوبولوجية ، والكتلة ثلاثية النوى رباعية الهيدريدو.